J Mater Sci: Mater Med (2009) 20:33–44
DOI 10.1007/s10856-008-3540-0

Synthesis and characterization of tyramine-based hyaluronan hydrogels

Aniq Darr · Anthony Calabro

Received: 3 April 2008 / Accepted: 10 July 2008 / Published online: 31 July 2008

Abstract Hyaluronan is particularly attractive for tissue engineering and repair because it: (1) is a normal component of the extracellular matrices of most mammalian tissues; (2) contributes to the biological and physical functions of these tissues; and (3) possesses excellent biocompatibility and physiochemical properties. In the present study, we characterize a two-step enzymatic cross-linking chemistry for production of tyramine-based hyaluronan hydrogels using fluorophore-assisted carbohydrate electrophoresis, enzymatic digestion, and spectroscopy including absorbance, fluorescence and ^{1}H NMR. Substitution on hyaluronan of tyramine and other adducts from unproductive side reactions depends on the molar ratio of tyramine to carbodiimide used during the substitution (step 1) reaction. Results indicate that relatively low tyramine substitution is required to form stable hydrogels, leaving the majority of hyaluronan disaccharides unmodified. Sufficient native HA structure is maintained to allow recognition and binding by b-HABP, a HA binding complex typically found in normal cartilage biology. Hydrogels were formed from tyramine-substituted hyaluronan through a peroxidase-dependent cross-linking (step 2) reaction at hyaluronan concentrations of 2.5 mg/ml and above. Uncross-linked tyramine-substituted hyaluronan was characterized after hyaluronidase SD digestion. Cross-linked hydrogels showed increased resistance to digestion by testicular hyaluronidase and hyaluronidase SD with increasing hyaluronan concentration. Cells directly encapsulated within the hydrogels during hydrogel cross-linking remained metabolically active during 7 days of culture similar to cells cultured in monolayer.

A. Darr · A. Calabro (✉)
Department of Biomedical Engineering, Orthopaedic Research Center, Lerner Research Institute, Cleveland Clinic Foundation, 9500 Euclid Avenue, Cleveland, OH 44195, USA
e-mail: calabra@ccf.org

A. Darr
Department of Biomedical Engineering, Case Western Reserve University, Cleveland, OH 44106, USA

1 Introduction

The ability to repair or regenerate tissue has been attempted by many laboratories through the utilization of three dimensional cell-scaffold constructs [1–3]. A variety of molecules have been utilized as scaffold materials, both natural and synthetic, in an attempt to provide a biologically compatible mechanical support for three dimensional tissue growth and differentiation. An ideal scaffold promotes growth of tissue, eventually resulting in replacement of the scaffold with healthy, functional tissue. Ideally, the scaffold facilitates this process by providing appropriate cell adhesion and differentiation signals that allow for maintenance of cell phenotype and promotion of native extracellular matrix (ECM) synthesis [3]. The facilitation process is dependent on the chemical and physical properties of the material chosen as the scaffold.

Hyaluronan, also known as hyaluronic acid (HA), is a glycosaminoglycan that has historically been considered a readily available and desirable scaffold material for tissue engineering applications. In tissues, HA plays a central role in many normal biologic processes through its interaction with cell receptors and other ECM molecules [4], and as a structural molecule, HA provides tissues with many of their physiomechanical properties [5]. As such, HA is readily synthesized and metabolized by a wide variety of cell and tissue types via normal physiological pathways [4]. Structurally, HA is composed of a repeat disaccharide of

glucuronic acid (glcA) and *N*-acetylglucosamine (glcNAc) linked by a β1,3-glycosidic bond (see structure, Fig. 1a) [4]. For each HA chain, this simple disaccharide is repeated up to 10,000 times ($N = 10{,}000$ in Fig. 1a) with each repeat disaccharide linked by a β1,4-glycosidic bond [4]. Due to its conservation from bacteria to mammals, and its ubiquitous distribution as a naturally occurring ECM molecule in almost all mammalian tissues, HA has been shown to be non-immunogenic, non-toxic and non-inflammatory [6, 7].

The chemical modification of HA has focused on its two principal functional groups, hydroxyl groups and carboxyl groups [8]. These groups have been utilized in a number of chemistries including: divinylsulfone [9], esterification [10], and carbodiimide mediated reactions [11]. These techniques are used to cross-link HA to form hydrogels with dynamic physical properties, depending on the extent and type of modification, but commonly involve the use of biologically incompatible chemistries leading to toxicities that result in a loss of cell and tissue viability if cross-linked in vivo.

Overcoming these complications has been a major focus in the development of advanced chemistries for HA hydrogel formation that are more biocompatible, such as photo-cross-linkable HA hydrogels [12], or those developed by Prestwich et al., which utilize disulfide [13] and thiol-reactive [14] groups to form synthetic ECM hydrogels for tissue engineering applications. Enzymatic cross-linking methodologies have emerged as an alternative pathway to overcome the difficulties associated with chemical cross-linking methods. Transglutaminase has been used to develop hydrogels from materials such as poly ethylene glycol [15], collagen [16], gelatin [17] and polypeptides [18]. Factor XIII has also recently been used to develop a peptide-PEG hydrogel [19]. In recent years, biomaterials have been formed through the cross-linking of tyramine conjugated polymers using horseradish peroxidase (HRP) in an attempt to maintain biocompatibility and provide the ability to cross-link in vivo. Examples of this chemistry include HRP cross-linked alginate [20], dextran [21], carboxymethylcellulose [22], and polyaspartic acid [23, 24].

HRP mediated cross-linking of tyramine adducts has also been used by our group [25, 26] and others [27] to form HA hydrogels. We have previously shown the ability to cross-link the tyramine-based HA (TB-HA) hydrogels in vivo using a canine model to treat functional mitral regurgitation [26], and have shown the TB-HA hydrogels to resist in vivo degradation for 8 weeks with minimal immune response using a subcutaneous rat model [25]. In this manuscript, we describe in detail the method for synthesis and characterization of the TB-HA hydrogels including possible side reactions. Furthermore, we provide in vitro data that supports our previous observations of in vivo biocompatibility of the HRP cross-linking reaction [26], and resistance to in vivo degradation [25]. Together these properties provide the potential for the use of the TB-HA hydrogels in a number of tissue engineering and repair strategies.

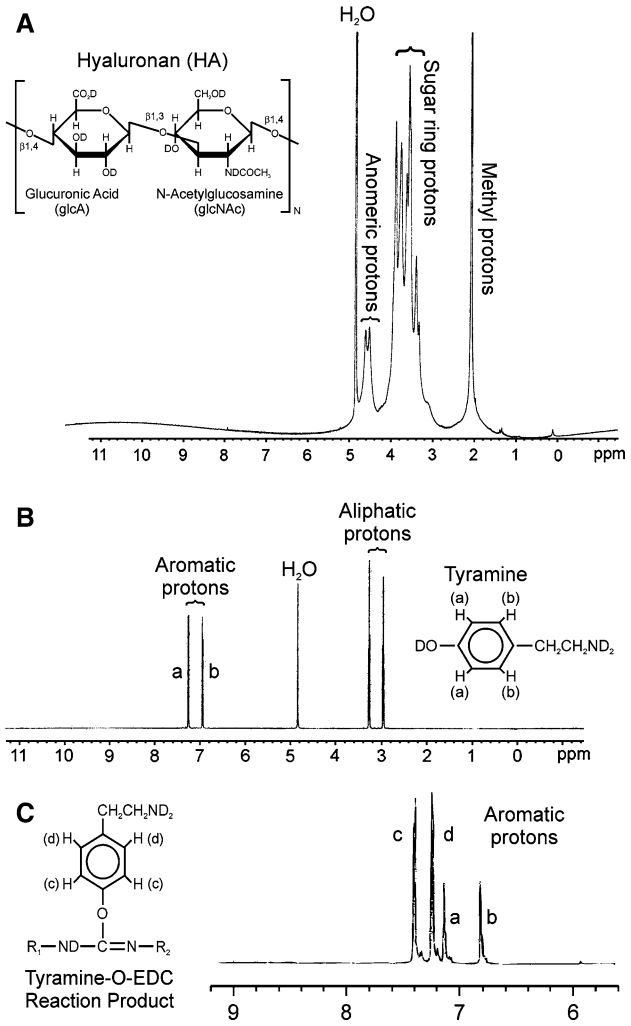

Fig. 1 The ^{1}H NMR spectra for (**a**) HA and (**b**) tyramine are shown along with schematics of their chemical structures. (**c**) The aromatic region for the ^{1}H NMR spectrum of the reaction products of tyramine and EDC in water at a molar ratio of 1 (1×) along with a schematic of the chemical structure for the tyramine-O-EDC reaction product. Proton assignments are indicated between schematics and spectra. The peak assignments between protons a and b in (**b**) and protons c and d in (**c**) are for purposes of simplicity only, and may be reversed

2 Materials and methods

2.1 Materials

Hyaluronan, sodium salt (molecular weight average >1 million Daltons), sodium hydroxide (NaOH), and

2-(*N*-morpholino)ethanesulfonic acid (MES) were purchased from Fisher Chemicals. 1-Ethyl-3-(3-dimethylaminopropyl)carbodiimide (EDC), *N*-hydroxysuccinimide (NHS), tyramine hydrochloride, sodium chloride, type II horseradish peroxidase (HRP), hydrogen peroxide, bovine testicular hyaluronidase, 10× insulin–transferrin–selenium (ITS) supplement and a hexokinase-based glucose assay (HK kit) were purchased from Sigma (St. Louis, MO). Hyaluronidase SD (*Streptococcus dysgalactiae*) and biotinylated hyaluronan binding protein (b-HABP) were purchased from Seikagaku Corporation (Tokyo, Japan). 2-Aminoacridone was purchased from Molecular Probes, Inc. (Eugene, Oregon). Eagle minimum essential medium (EMEM), fetal calf serum (FCS) and 10× phosphate buffered saline (PBS) were purchased from Invitrogen Corporation (Carlsbad, CA). Tissue Tek O.C.T. frozen tissue sectioning medium was purchased from Sakura USA (Torrance, CA). Fluorescein isothiocyanate-streptavidin and Vectashield were purchased from Vector Laboratories (Burlingame, CA).

2.2 Synthesis of tyramine-substituted hyaluronan (TS-HA)

Hyaluronan was dissolved at 1 mg/ml based on hexuronic acid assay [28] in 250 mM MES containing 150 mM NaCl and 75 mM NaOH (pH_{start} 5.75, pH_{end} 6.25). A 10 fold molar excess of tyramine to the moles of carboxyl groups (glcA residues) in HA was added. Tyramine coupling was initiated by the addition of either a 0 (0×), 0.1 (0.1×) or 1 (1×) fold molar amount of EDC relative to the moles of tyramine, and the reaction mix was stirred continuously at room temperature for 24 h. A 1/10th molar amount of NHS relative to the amount of EDC was added to the reaction mixture with the EDC. Macromolecular TS-HA was recovered by exhaustive dialysis versus 150 mM NaCl and then ultrapure water. Finally, the dialyzed TS-HA was lyophilized, and then dissolved to the desired working concentration in PBS or ultrapure water as appropriate.

2.3 Formation of tyramine-based hyaluronan (TB-HA) hydrogels

Lyophilized TS-HA was resuspended at concentrations of up to 25 mg/ml in 1× PBS or ultrapure water, and allowed to fully hydrate for 24 h at 4°C with repeated vortex mixing. Just prior to cross-linking, HRP was added to a final concentration of 10 U/ml and thoroughly mixed by vortex. For all analyses except the enzymatic digestion studies described in Fig. 8, the formation of TB-HA hydrogels from various TS-HA solutions containing HRP was initiated by introduction by vortex mixing of 40 µl of 0.03% hydrogen peroxide per 1.0 ml of TS-HA solution. For the enzymatic digestion studies, cylindrical plugs (~7.1 mm in diameter, ~3 mm in thickness) at HA concentrations of 6.25, 12.5, and 25 mg/ml were formed using a custom built polycarbonate mold, and the cross-linking technique described below. The mold was filled with replicate aliquots of the desired TS-HA formulation containing 10 U/ml of HRP and frozen on dry ice. The mold was then immersed in an excess (200 ml) of room temperature hydrogen peroxide solution (0.03%). This immersion allowed for thawing of the frozen hydrogel plugs and dityramine cross-linking throughout the plugs as a result of the outside-in diffusion of peroxide from the immersion solution. Cross-linking was determined to be complete once the last visual evidence of ice had melted at the center of the forming hydrogel plugs (~5 min). The mold was then removed blotted dry, and the hydrogel plugs were removed for enzymatic digestion.

2.4 Spectrophotometric analysis of TS-HA preparations

The amount of tyramine adduct covalently bound within TS-HA prepared with EDC to tyramine ratios of 0 (0×), 0.1 (0.1×) and 1 (1×) was calculated by measuring the tyramine absorbance at 275 nm of a 1 mg/ml TS-HA solution in ultrapure water based on hexuronic acid assay [28] using a SpectraMax Plus Spectrophotometer (Molecular Devices, Inc.). The absorbance measured was compared to a tyramine standard curve composed of 20, 40, 60, 80, and 100 µg/ml of tyramine in ultrapure water. The percent substitution of tyramine within a TS-HA preparation was then calculated from the molar ratio of covalently bound tyramine residues to total carboxyl groups on HA, based on hexuronic acid assay [28].

2.5 ^{1}H NMR analysis of TS-HA

Lyophilized TS-HA prepared with EDC to tyramine ratios of 0 (0×), 0.1 (0.1×) and 1 (1×) were rehydrated in deuterated water, lyophilized and rehydrated again in deuterated water. ^{1}H NMR (600 MHz) was performed using a Bruker solution state spectrometer (Bruker, Billerica, MA). Assignments were made using standards for each of the reagents used in the tyramine substitution (step 1) reaction with the signals for aromatic protons assigned at $\delta = 6.5$–7.5 ppm, anomeric protons at $\delta = 4.0$–4.5 ppm, sugar ring protons at $\delta = 3.0$–4.0 ppm, and aliphatic protons at $\delta = 1.0$–2.0 ppm.

2.6 Detection of fluorescent dityramine bridges

Two hundred microliters of TS-HA (5 mg/ml) prepared with an EDC to tyramine ratio of 1 (1×) in ultrapure water was cross-linked in a 96 well fluorescence plate as

described above. After 24 h to ensure complete cross-linking, the emission and excitation wavelengths for the resulting cross-linked TB-HA hydrogel was determined using a Gemini Spectrophotometer (Molecular Devices, Inc.).

2.7 Fluorophore-assisted carbohydrate electrophoresis (FACE)

For FACE analysis, 50 nanomoles of uncross-linked TS-HA and cross-linked TB-HA hydrogel prepared with EDC to tyramine ratios of 0 (0×), 0.1 (0.1×) and 1 (1×) were processed for FACE analysis as described previously [29–31]. Briefly, aliquots were extensively digested with hyaluronidase SD to digest the unsubstituted portions of HA to its limit, repeat disaccharide (ΔDiHA) and the portions of HA modified with adducts from the tyramine substitution (step 1) reaction to limit HA oligosaccharides. These saccharides were then tagged through their reducing aldehydes with the fluorophore, 2-aminoacridone (AMAC), which provides a molar reporter for each saccharide. The AMAC-tagged saccharides were then separated on polyacrylamide gels using a borate buffer, the gels imaged, and the amounts of unsubstituted HA disaccharides (ΔDiHA) quantified as previously described [29–31]. The relative mobility of the unsubstituted HA disaccharide was confirmed using AMAC-tagged ΔDiHA standard.

2.8 Enzymatic digestion of TB-HA hydrogels

TB-HA hydrogels plugs (~7.1 mm in diameter, ~3 mm in thickness) were prepared in 1× PBS at concentrations of 6.25, 12.5 and 25 mg/ml as described above, and then digested with either testicular hyaluronidase, or hyaluronidase SD as follows. Two replicate hydrogel plugs at each HA concentration were placed in a 1.5 ml microcentrifuge tube, and 900 µl of 1× PBS containing either 20 units of testicular hyaluronidase or 0.5 unit of hyaluronidase SD was added. Samples were placed in a 37°C water bath for 24 h and agitated for 30 seconds every 4 h. Following the 24 h digestion, the amount of HA released into solution was determined using hexuronic acid content [28].

2.9 Cell culture

Immortalized rat chondrocytes were isolated as previously described [32]. Cells (3×10^6) were suspended in duplicate 1 ml aliquots of 1× PBS containing HRP and TS-HA (5 mg/ml) prepared with EDC to tyramine ratios of either 0.1 (0.1×) or 1 (1×), and then cross-linked in a 1.5 ml sterile microcentrifuge tube as described above. After 10 min of cross-linking, the hydrogels with embedded cells were washed in PBS for 5 min. Following the wash, the cell-hydrogel construct was cut into 2 mm thick slices. The entire sliced construct, containing 3×10^6 cells, was cultured in a 35 mm dish containing 3 ml of medium (EMEM containing 1× ITS) under standard conditions for 7 days with daily medium changes. Control 35 mm dishes containing 3×10^6 cells in monolayer were cultured concurrently under standard conditions for 7 days with medium changes every day. Glucose utilization with time in culture as measured by standard hexokinase assay (Sigma) was used as an indicator of cell viability.

2.10 Biotinylated-hyaluronan binding protein (b-HABP) staining of TB-HA hydrogel

A 100 µl aliquot of 5 mg/ml TS-HA (1×) was spread between two standard microscope slides, and cross-linked by submersion in a 0.03% hydrogen peroxide solution. The resulting TB-HA hydrogel sheet was stained with b-HABP as follows [33, 34]. The hydrogel sheet was first incubated with a 50% FCS/50% PBS solution for 1 h at 4°C, and then washed with 1× PBS. The hydrogel sheet was next incubated at 4°C overnight with b-HABP (5 µg/ml), and then washed with 1× PBS. Finally the hydrogel sheet was incubated with fluorescein labeled streptavidin at room temperature for 1 h, and then washed with 1× PBS. The stained hydrogel sheet was affixed to a microscope slide in Vectashield mounting medium and analyzed by a Leica TCS-NT laser-scanning confocal microscope.

3 Results and discussion

3.1 HA modification (step 1: tyramine substitution reaction)

The formation of amide bonds between the free carboxyl groups on HA molecules and the free amine groups on tyramine molecules (see structures, Fig. 1) are made through conventional carbodiimide chemistry [35, 36]. The reaction involves activation of the carboxyl group with EDC to create a reactive *O*-acylisourea intermediate [35]. Nucleophilic attack by the electron rich amine group of tyramine on the now electron deficient carbonyl carbon of glcA creates the desired amide bond covalently linking tyramine to the HA molecule (Fig. 2). The EDC is converted to the unreactive acylurea form of EDC. *N*-Hydroxysuccinimide is included as a catalyst to facilitate the EDC reaction by formation of an active ester, minimizing side reactions that generate adducts other than tyramine on the TS-HA [35]. These additional adducts do not participate in the subsequent cross-linking reaction described below, and are thus considered unproductive and undesirable [35].

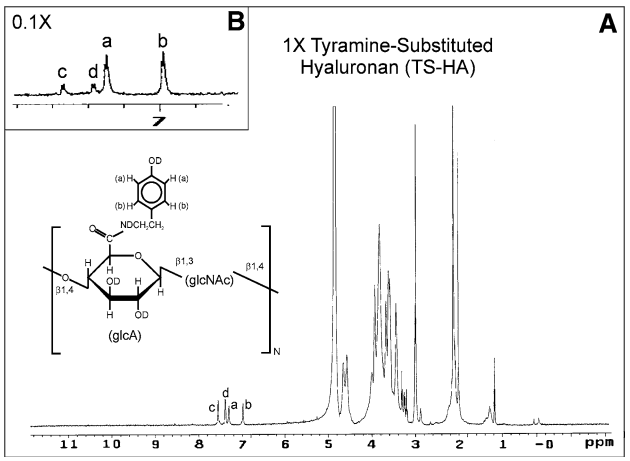

Fig. 2 (**a**) ^{1}H NMR spectrum for tyramine-substituted HA (TS-HA) synthesized using a molar ratio of EDC to tyramine of 1 (1×) as described in methods along with a schematic of its chemical structure. (**b**) Aromatic region of the ^{1}H NMR spectrum for TS-HA prepared using a molar ratio of EDC to tyramine of 0.1 (0.1×). Protons are as assigned in Fig. 1

Unproductive adducts occur as a result of two different side reactions. The first is typical of conventional carbodiimide chemistry. The reactive *O*-acylisourea intermediate described above undergoes intramolecular rearrangement to form *N*-acylurea adducts on HA (Fig. 3a). Two distinct adducts are possible due to the asymmetric nature of the EDC molecule. The *N*-acylurea adduct has been shown in vivo to be lost with time from HA by a non-enzymatic hydrolysis reaction, which regenerates the native HA carboxyl groups and releases EDC in its acylurea form [11, 37]. This may be beneficial for applications to wound repair in that the acylurea form of EDC has been shown to be anti-inflammatory, and able to inhibit abdominal sepsis [38, 39].

The second side reaction is unique to carbodiimide chemistry involving molecules containing a hydroxyphenyl group such as tyramine. Reaction of EDC directly with the hydroxyphenyl group on tyramine (whether free in solution or already covalently bound to HA through its amine group) forms tyramine-O-EDC adducts on HA (Fig. 3b). Again two distinct adducts are possible due to the asymmetric nature of the EDC molecule. When formed from tyramine free in solution, both of these chemical species retain their free amine group, which can participate in the same nucleophilic attack of the reactive *O*-acylisourea intermediate as described above for tyramine with subsequent covalent attachment to carboxyl groups on HA. However, unlike tyramine, the tyramine-O-EDC adduct is unable to participate in the enzymatic cross-linking reaction described below as it has no extractable phenolic hydroxyl hydrogen atoms (now occupied by EDC). The evidence for the existence of these unproductive adducts on TS-HA is provided below.

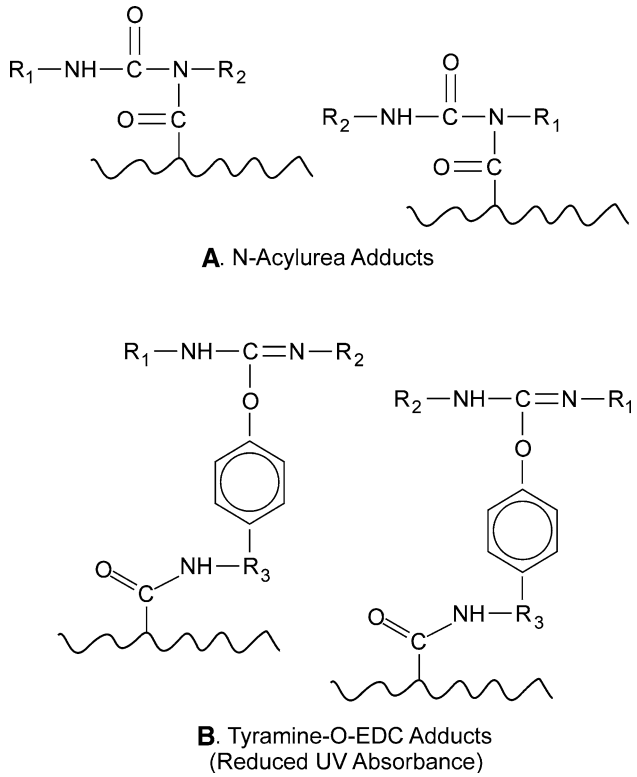

Fig. 3 Schematics of potential unproductive reaction adducts on TS-HA: (**a**) *N*-acylurea adducts; and (**b**) tyramine-O-EDC adducts. $R_1 = CH_2CH_3$, $R_2 = CH_2CH_2CH_2NH^+(CH_3)_2Cl^-$ and $R_3 = CH_2CH_2$

3.1.1 Measurement of percent tyramine substitution on HA

Recovery after dialysis was greater than 95% for TS-HA prepared with all EDC to tyramine ratios used in this study based on hexuronic acid assay [28] (data not shown). This assay, which is used routinely for quantification of glycosaminoglycans such as HA, detected both unsubstituted and substituted HA equally presumably due to cleavage of the HA adduct bond during heating to 100°C in the concentrated sulfuric acid used in this assay. The percent tyramine substitution on HA prepared with EDC to tyramine ratios of 0 (0×), 0.1 (0.1×) and 1 (1×) following the carbodiimide-mediated reaction were calculated from the molar ratio of covalently bound tyramine residues to total carboxyl groups on HA. Tyramine, by virtue of its hydroxyphenyl group, absorbs UV light with an absorbance maximum of 275 nm. Therefore the molar concentration of tyramine associated with a 1 mg/ml TS-HA preparation can be determined by measuring its absorption at 275 nm (Fig. 4b) relative to a tyramine standard curve (Fig. 4c, d). Values for the percent substitution of tyramine in the 0×, 0.1×, and 1× TS-HA preparations were 0, 1.7 and 4.7%, respectively. The relatively low percent tyramine substitution presumably accounts for the high percent recoveries

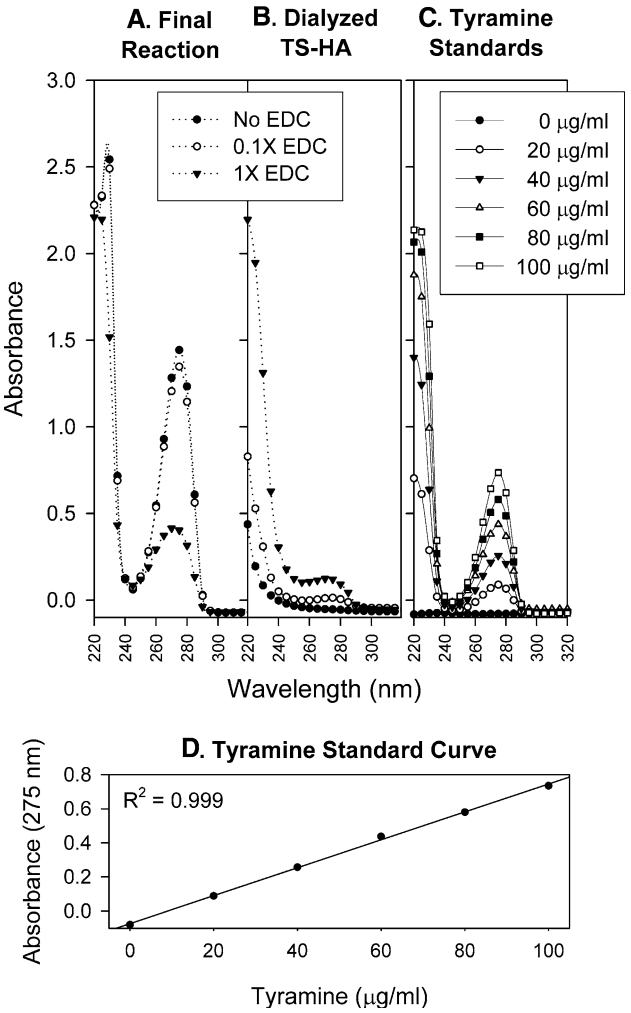

Fig. 4 Spectrophotometric absorbance spectra (220–320 nm) for (**a**) final (24 h) tyramine substitution reaction mixtures prior to dialysis, (**b**) dialyzed 1 mg/ml TS-HA preparations prepared with EDC to tyramine ratios of 0 (0×), 0.1 (0.1×) and 1 (1×), and (**c**) tyramine standards. Absorbance vs. concentration curve (**d**) for tyramine standards derived from the spectra in (**c**) using absorption values at the tyramine absorbance maximum of 275 nm. Absorbance values at 275 nm from the spectra in (**b**) were used along with standard curve (**d**) to calculate the percent tyramine substitution in 1 mg/ml TS-HA preparations

observed as much of the hydrophilic nature of HA is preserved.

Tyramine absorbance at 275 nm was used to detect the formation of the tyramine-O-EDC adducts described above (Fig. 3b). In Fig. 4a, the absorbance at 275 nm of the final reaction mixture decreases proportional to increasing EDC concentration as more tyramine reacts with the EDC to form the structures in Fig. 3b. Therefore, while all three final reaction mixtures, in which small molecular weight reactants have not yet been removed by dialysis, contain the same tyramine concentration, the absorbance at 275 nm decreases with increasing EDC concentration. This has been confirmed by reacting EDC and tyramine alone in solution and observing the same loss of absorbance at 275 nm (data not shown).

3.1.2 ^{1}H NMR spectroscopy of TS-HA

^{1}H NMR spectroscopy was used to characterize adducts on HA as a result of the carbodiimide-mediated (step 1) reaction with the results shown in Figs. 1 and 2. A comparison of the spectra for unsubstituted HA (Fig. 1a) and TS-HA (Fig. 2a) shows signals for the anomeric protons (one per monosaccharide at ~4.6 ppm), sugar ring protons (four per monosaccharide between 3.2 and 4.0 ppm), and methyl protons of the *N*-acetyl group (3 per disaccharide, at ~2 ppm) expected from both molecules [40]. In addition, the TS-HA spectra show additional peaks, not seen in the unsubstituted HA, which represent signals from protons on adducts added during the carbodiimide reaction and identified as follows.

In the spectrum for the tyramine reagent (Fig. 1b), the distinctive signals for both pairs of aromatic ring protons (a pair and b pair between 6.9 and 7.3 ppm) and aliphatic side chain protons between 2.9 and 3.3 ppm are easily identified. These same a/b signals are seen in the spectra for purified TS-HA confirming the presence of the tyramine adduct on TS-HA (Fig. 2). It should be noted that the same a/b signal is seen whether tyramine is covalently bound or not. It is important that during purification (dialysis) of the TS-HA, sufficient salt such as NaCl be added to the reaction and initial dialysis buffers, otherwise non-covalently bound tyramine molecules, in the form of counterions with HA carboxyl groups, contaminate the final product (data not shown). These non-covalently bound tyramine molecules, while able to form dityramine cross-links as a result of the HRP reaction described below, inhibit formation of stable dityramine bridges between covalently bound tyramine adducts on TS-HA chains, weakening the resulting hydrogels. The presence of contaminating non-covalently bound tyramine may account for the higher percent tyramine substitution values (9%) reported by Kurisawa et al. [27] as well as the less stabile nature of their hydrogels in vitro and in vivo (see below) compared to those reported in this study.

In the spectra for the TS-HA (Fig. 2), there are two additional aromatic signals (peaks c and d) at higher δ values (above 7.3 ppm) than observed for tyramine alone. These same c/d signals are seen in the spectrum in Fig. 1c for the products of the reaction of tyramine and EDC in the absence of any other reagents (water only). These additional signals result from the formation of the tyramine-O-EDC adducts depicted in Fig. 3b with the c/d signals arising from the two pairs of aromatic ring protons (c pair and d pair) shown in Fig. 1c. The substitution of the EDC for the exchangeable phenolic proton on tyramine shifts the

signal for the aromatic ring protons of the tyramine-O-EDC adduct to higher δ values, and drastically reduces the absorbance of the tyramine-O-EDC at 275 nm producing results similar to the data in Fig. 4a (data not shown). As stated above Kurisawa et al. [27] reported a percent tyramine substitution on HA of 9% based on NMR, but did not show any spectra, so it is not known whether they included all of the aromatic signal as tyramine in their calculations.

A molar ratio of EDC to tyramine of 1 was used to generate the spectra in both Figs. 1c and 2a. In both, the relative amounts of the tyramine-O-EDC to tyramine are similar with more tyramine-O-EDC adduct than tyramine adduct. Decreasing the molar ratio of EDC to tyramine from 1 to 0.1 results in less tyramine substitution on HA, but also increases the relative amount of tyramine adduct above that of the tyramine-O-EDC adduct (Fig. 2b). Together, the results in Figs. 1, 2 and 4 confirm the presence of both tyramine and tyramine-O-EDC on TS-HA and validate the use of absorbance at 275 nm for determination of the percent tyramine substitution only on TS-HA. Signals below 4.0 ppm in the spectrum for TS-HA (Fig. 2a) not present in the spectra for unsubstituted HA (Fig. 1a) represent the aliphatic protons on adducts containing tyramine and EDC on TS-HA.

3.2 Hydrogel formation (step 2: enzymatic cross-linking)

The peroxidase catalyzed oxidation of tyramine on TS-HA to dityramine (cross-linking reaction) forming TB-HA hydrogels is shown in Fig. 5 [41]. Peroxidase in the presence of hydrogen peroxide preferentially extracts the phenolic hydroxyl hydrogen atom from tyramine leaving the phenolic hydroxyl oxygen with a single unshared electron, a reactive free radical. The free radical isomerizes to one of the two equivalent ortho-position carbons, and then two such structures dimerize to form a covalent bond cross-linking the structures, which after enolizing, generates dityramine. The formation of multiple such dityramine cross-links between adjacent HA molecules results in formation of a three dimensional network, i.e. a hydrogel.

TB-HA hydrogels were successfully formed through cross-linking of both 0.1× and 1× TS-HA formulations in concentrations as low as 2.5 mg/ml HA with the initiation of cross-linking occurring immediately upon mixing to introduce the hydrogen peroxide. During all cross-linking reactions, hydrogel formation occurred in less than 2 s, which is consistent with previously published values for gelation times using these concentrations of HRP and peroxide [21–24, 27]. Low concentration hydrogels were transparent and became increasingly opaque with increasing TS-HA concentration. All hydrogels formed were of sufficient mechanical strength to hold their shape, but the relative rigidity increased with increasing TS-HA concentration.

Of note is that the preferred substrates for HRP are phenolic structures such as found in tyramine, and that the normal in vivo function in the plant of HRP of lignification (or cross-linking of plant cell walls, a natural hydrogel) involves structures similar to those of tyramine [42]. As an enzyme, peroxidase must be first activated by peroxide before the peroxidase can use tyramine adducts on TS-HA as substrate. The activated peroxidase then must sequentially catalyze the formation of two free radicals (such as the two tyramine free radicals needed to form one dityramine bridge, Fig. 5) before regenerating the porphyrin ring of the peroxidase enzyme [42]. The peroxidase enzyme is then ready to be activated again by the peroxide and begin another cycle of catalysis. Thus TS-HA in the presence of either the peroxide or peroxidase alone does

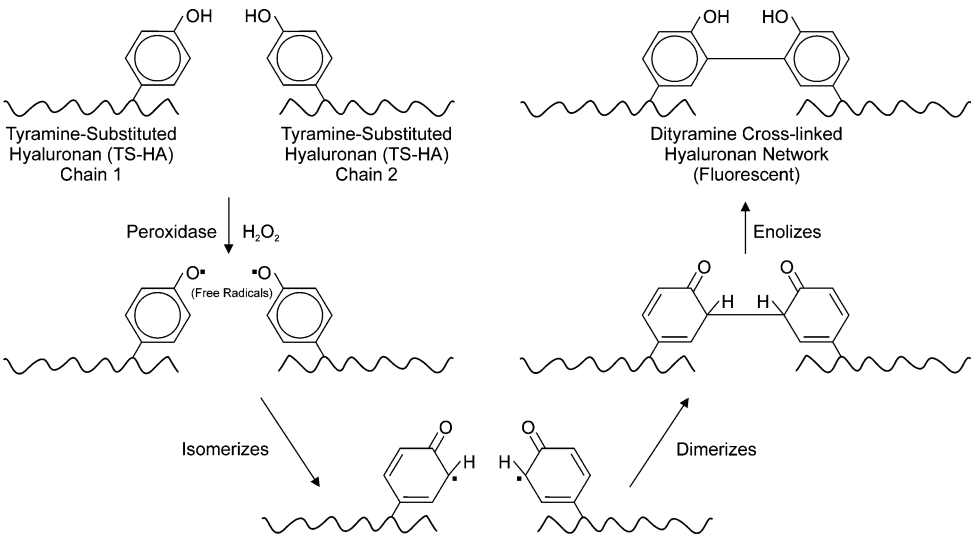

Fig. 5 Schematic representation of the proposed mechanism for peroxidase catalyzed oxidation of tyramine on TS-HA to form dityramine cross-links (adapted from [41])

not undergo the cross-linking reaction to a hydrogel. Interestingly, as the hydrogel forms thereby preventing diffusion of the macromolecular HRP, formation of tyramine free radicals (and thus further cross-linking) may continue to occur over relatively short molecular distances independent of tyramine binding at the HRP active site. This is possible through free radical intermediates generated as water molecules bind to the active site of HRP and then diffuse away allowing a more complete cross-linking than otherwise expected [42].

3.3 Measurement of the fluorescent dityramine bridges in TB-HA hydrogels

Unlike tyramine, the dityramine cross-link fluoresces blue-green upon exposure to UV light. TB-HA hydrogels displayed an excitation maximum of 285 nm and an emission maximum of 415 nm (Fig. 6). Their intrinsic fluorescence is used to assess both the initiation of the cross-linking reaction and its propagation throughout the total volume of the hydrogel.

3.4 FACE analysis of TB-HA hydrogels

The FACE methodology [29–31] was previously developed by the senior author to quantify and characterize glycosaminoglycans, such as HA, through the electrophoretic separation of fluorescently (AMAC) tagged glycosaminoglycan products following enzymatic digestion. FACE can be used in this context to identify after hyaluronidase SD digestion: 1) the unsubstituted (native) HA repeat disaccharides (ΔDiHA); and 2) HA oligosaccharides with attached adducts. Hyaluronidase SD is an eliminase that normally irreversibly and completely cleaves unsubstituted HA to a limit digest of ΔDiHA disaccharides under the reaction conditions used in this study. Figure 7 shows an oversaturated image of a representative FACE gel of AMAC-tagged hyaluronidase SD digestion products of: a) uncross-linked TS-HA prepared with EDC to tyramine ratios of 0 (0×), 0.1 (0.1×) and 1 (1×); and b) cross-linked TB-HA hydrogels synthesized from 0.1× and 1× TS-HA. Only after hyaluronidase SD digestion are fluorescently tagged saccharides visualized as in Fig. 7. The same amount of total HA based on hexuronic acid assay [28] was loaded per lane. The relative mobility of AMAC-tagged ΔDiHA was confirmed using a commercially available standard.

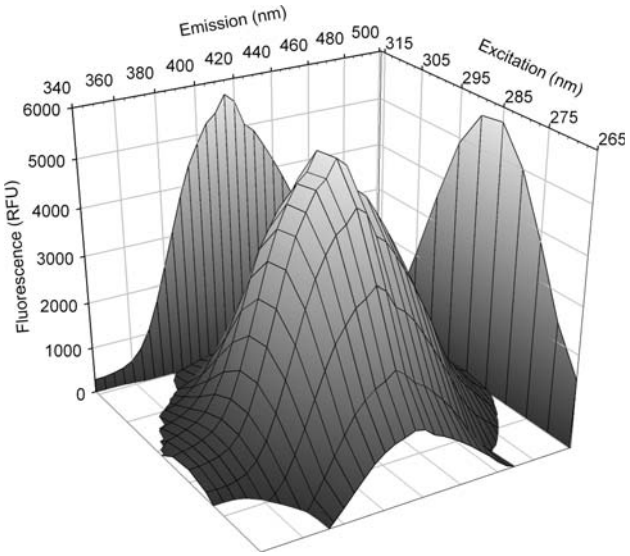

Fig. 6 Fluorescence as a function of excitation and emission wavelength for cross-linked TB-HA hydrogel

3.4.1 Detection of unsubstituted HA disaccharides (ΔDiHA)

The relative amounts of ΔDiHA for the 0.1× and 1× TS-HA based on quantification of a properly saturated image of the gel in Fig. 7 were between 96–100 and 62–69%, respectively compared to the 0× TS-HA. Thus the amount of measurable ΔDiHA decreased with increasing EDC to tyramine ratio as a result of increased substitution of the HA with tyramine (see Fig. 2) and other adducts (see Fig. 3). Based on the expected specificity of the hyaluronidase SD enzyme for an unsubstituted HA disaccharide on both sides of a cleavable glycosidic bond, the estimation of the amount of unsubstituted HA disaccharide by FACE is an under estimation as it is expected that at least two

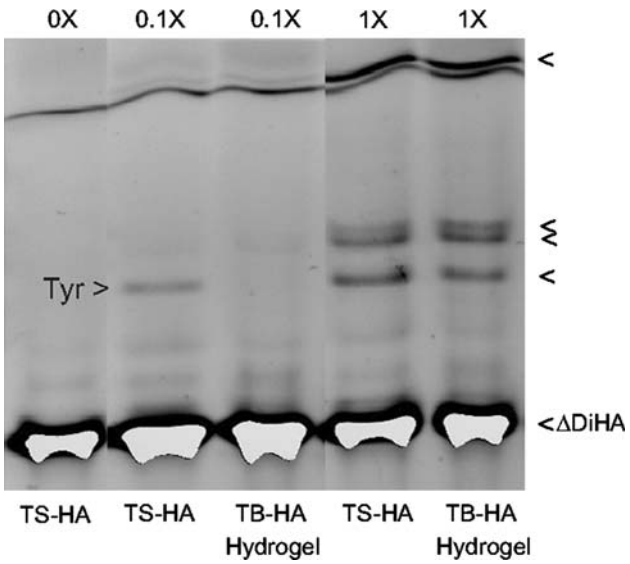

Fig. 7 Digital images of FACE gels showing the relative mobility of AMAC-derivatized products after hyaluronidase SD digestion of TS-HA or cross-linked TB-HA hydrogel prepared with EDC to tyramine ratios of 0 (0×), 0.1 (0.1×) and 1 (1×). Digital image is over exposed for the ΔDiHA bands so as to allow visualization of substituted HA oligosaccharide bands

unsubstituted HA molecules (ΔDiHA) bookend each substituted HA disaccharide after enzymatic digestion. Thus, an approximately 70% recovery of ΔDiHA for the 1× TS-HA would correspond to a substitution rate of 10% of the total HA disaccharides. An estimate of 10% substitution is consistent with the measured percent tyramine substitution for the 1× TS-HA of 4.7% based on absorbance at 275 nm if then combined with a slightly higher molar amount of tyramine-O-EDC adduct based on the NMR results (Fig. 2).

3.4.2 Detection of substituted HA oligosaccharides

Based on the NMR data for the 0.1× TS-HA (Fig. 2b), tyramine is predicted as the major adduct present on HA, and only one new minor band (Tyr >) not present in the 0× TS-HA lane is seen in the 0.1× TS-HA lane in Fig. 7. This band is tentatively identified as arising from the desired tyramine adduct containing digestion product (see schematic, Fig. 2a). This is supported by the absence of this band in the corresponding 0.1× TB-HA hydrogel lane prepared from cross-linked 0.1× TS-HA, and the appearance of a new fluorescent blue band in the gel stacker in this lane. The fluorescent band is presumed to be composed of two HA oligosaccharides cross-linked by a fluorescent dityramine bridge. The fluorescent band was not imaged due to normal filtering of similar wavelengths of light generated by the UV light source during normal image capture. In contrast, four distinct minor bands (<) are seen in the 1× TS-HA lane consistent with the greater degree of non-tyramine adducts identified by NMR (Fig. 2a). The three slower moving bands are unchanged in intensity after cross-linking to 1× TB-HA hydrogel as expected of unproductive adducts (Fig. 3) unable to participate in the cross-linking reaction. The fastest moving band appears to co-migrate with the Tyr band, and it decreases in intensity upon cross-linking to hydrogel, but does not disappear completely as for the 0.1× sample. This implies either incomplete cross-linking of tyramine adducts, presumably for reasons of steric hindrance, or the presence of an unproductive adduct co-migrating with the tyramine adduct digestion product.

3.5 Enzymatic digestion of TB-HA hydrogels

The stabile nature of both the amide bond as a result of the tyramine substitution (step 1) reaction and the dityramine bridge carbon-carbon bond as a result of the peroxidase cross-linking (step 2) reaction are expected to provide a chemically stabile material presumably reliant on exogenous tissue hyaluronidases for in vivo scaffold degradation, and not simple hydrolysis. In Fig. 8, 6.25, 12.5, and 25 mg/ml TB-HA hydrogel plugs (inset) were digested at 37°C with excessive amounts of either mammalian testicular hyaluronidase (hydrolase) or bacterial hyaluronidase SD (eliminase). The amount of HA as measured by hexuronic acid assay [28] released into solution after 24 h and expressed as a percentage of the total plug concentration were similar independent of the enzyme used (Fig. 8). The resistance to digestion increased with increasing concentration. The 6.25 mg/ml gels showed the highest level of digestion, with 99.8 and 82.3% being released into solution for testicular hyaluronidase and hyaluronidase SD, respectively, while the 25 mg/ml gels showed the lowest level of digestion, with 30.3 and 30.2% being released for testicular hyaluronidase and hyaluronidase SD, respectively.

These results were in contrast to those reported by Kurisawa et al. [27], who showed complete digestion within 7 h for 16.6 mg/ml tyramine cross-linked HA hydrogels, under similar digestion conditions, although the

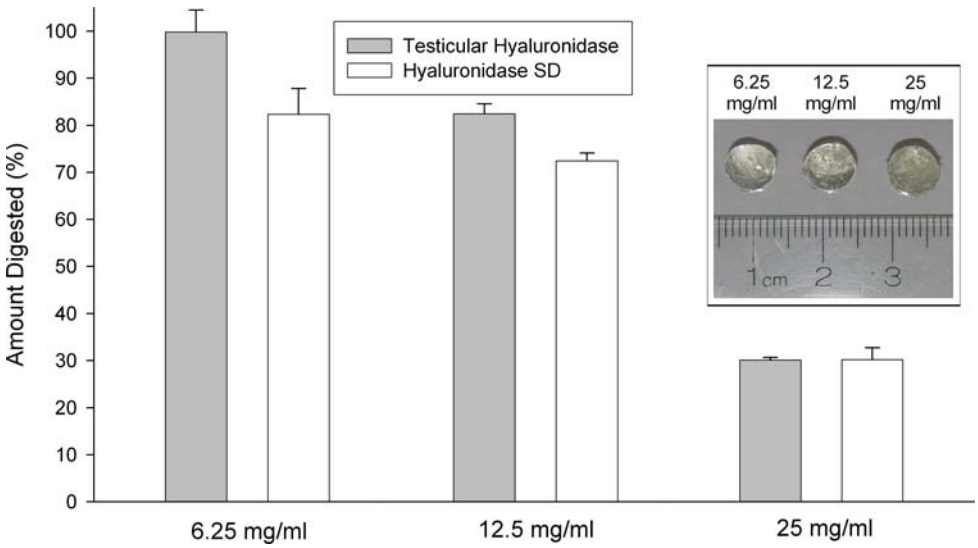

Fig. 8 Enzymatic digestion of cross-linked TB-HA hydrogels composed of 6.25, 12.5 and 25 mg/ml HA and digested with either testicular hyaluronidase or hyaluronidase SD. Inset shows TB-HA hydrogel plugs (~7.1 mm in diameter, ~3 mm in thickness) made from TS-HA and cross-linked at concentrations of 6.25, 12.5 and 25 mg/ml based on hexuronic acid assay [28]

type of hyaluronidase used was not stated. Additionally, Kurisawa et al. reported in vivo degradation of 50–100% of tyramine cross-linked HA hydrogels within 30 days in a subcutaneous rat model. In contrast, our previously work showed in vivo stability of our TB-HA hydrogels at 8 weeks, with little or no degradation [25]. As previously stated, the difference in results may be due to contamination of the hydrogels of Kurisawa et al. with non-covalently bound tyramine, and resulting hydrogels that are more susceptible to in vitro digestion and in vivo degradation. Another explanation for the difference in material properties is the exclusion of HRP from the tyramine substituted HA by Kurisawa et al. prior to cross-linking relying instead on diffusion of both HRP and peroxide for cross-linking. This may have limited cross-linking to the surface of the hydrogel volume as the macromolecular HRP, unlike the small molecular weight peroxide, would be inhibited from diffusing through the gel as it cross-linked. This would minimize, rather than maximize cross-linking, potentially resulting in a more lightly cross-linked hydrogel as compared to the method described in this study, which has the peroxidase thoroughly mixed with the TS-HA prior to cross-linking, and requires only diffusion of the low molecular weight peroxide to initiate cross-linking.

3.6 Biocompatibility of peroxidase cross-linking reaction and TB-HA hydrogels

The biocompatibility of the HRP cross-linking reaction was assessed by suspending freshly isolated immortalized chondrocytes [32] in 5 mg/ml TS-HA solutions prepared with EDC to tyramine ratios of 0.1 (0.1×) and 1 (1×), and then cross-linking the hydrogels in the presence of the cells. Glucose consumption as measured by hexokinase assay (Sigma) was used to assess cell viability, as well as adequate diffusion of oxygen, glucose and insulin through the hydrogel volume. During culture, chondrocytes appeared uniformly distributed when observed through a light microscope with the optical clarity of the hydrogels at 5 mg/ml allowing visualization throughout their volume. In Fig. 9, the results show that chondrocytes embedded in TB-HA hydrogels had essentially the same glucose consumption profiles over 24 h as the chondrocytes cultured in monolayer. This similarity continued for each 24 h period up to 7 days (only day 1 shown) indicating that the cells were metabolically active throughout the culture period and that both the cross-linking process and the TB-HA hydrogels themselves were not cytotoxic. It is interesting to note that HRP, a glycoprotein, has been shown to be protected from substrate radical inactivation by the ~20% N-linked oligosaccharides decorating its protein backbone. These oligosaccharides contain significant glcNAc, the same monosaccharide found in the repeat disaccharide structure of HA [42]. Thus under the appropriate conditions, glcNAc in HA may play a protective role for cells during the HRP cross-linking reaction. No statistically significant difference (*t*-test) was seen between cultures at 24 h. Differences were seen at 6, 8 and 12 h time points, presumably due to the lag in nutrient diffusion that exists for the hydrogel versus monolayer cultures (three dimensional vs. monolayer). The results indicate that oxygen, glucose, insulin and any other required medium factors diffuse through the TB-HA hydrogels at a rate that is not damaging to cell viability.

These results are not unexpected as not only HA, but the other molecules comprising the TB-HA hydrogels are all naturally occurring components of normal mammalian tissues, and as such are expected to contribute to the biocompatible nature of these biomaterials. Tyramine is the

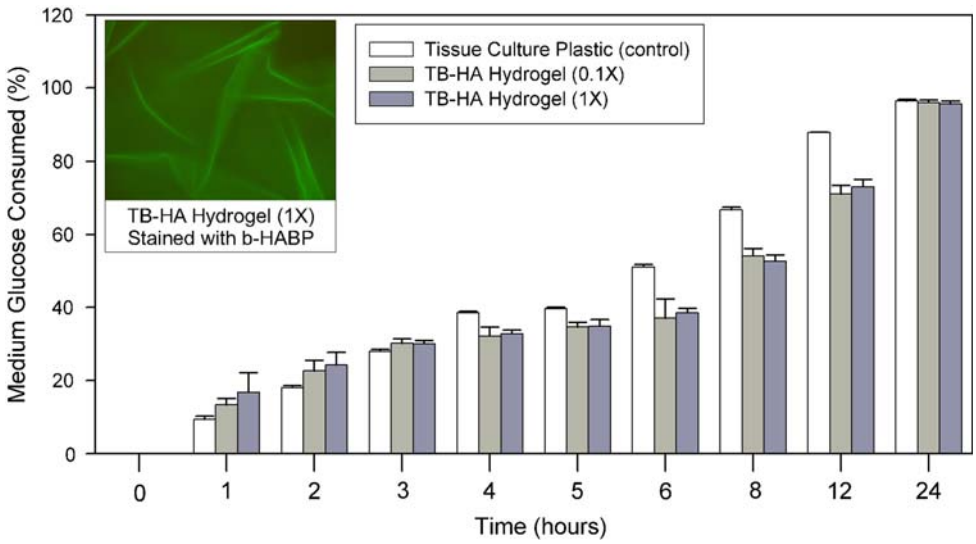

Fig. 9 Glucose consumption as a measure of cell viability versus time for cells embedded in TB-HA hydrogels (5 mg/ml) compared to cells cultured in monolayer on tissue culture plastic. Hydrogels cross-linked using TS-HA prepared with EDC to tyramine ratios of 0.1 (0.1×) and 1 (1×). Inset showing 5 mg/ml TB-HA hydrogel sheet stained with b-HABP

major neurotransmitter in insects, but in mammals is primarily an intermediate in the synthetic pathway of dopamine and norepinephrine, the two major neurotransmitters in mammals, and as such tyramine is present in brain tissue as a trace amine at only 1/100th the concentration of these neurotransmitters [43]. In mammals, tyramine is characterized as a neuromodulator with no post-synaptic excitability in the absence of neurotransmitter [43].

The dihydroxyphenyl bridges that result from the enzymatic cross-linking of tyramine to dityramine in the TB-HA hydrogels are also present in plant, insect and mammalian tissues. Where known, these bridges are formed as a result of the action of endogenous peroxidase activity on tyrosine residues in resident tissue proteins generating dityrosine bridges [44–46]. The structures of tyramine and tyrosine differ only in the presence of an α-carboxyl group on tyrosine. Peroxidase is ubiquitous throughout most mammalian tissues with peroxidase reactions similar to that in the TB-HA cross-linking reaction, a predictable feature at the site of wound repair where a tissue engineering approach might be employed [46, 47].

The potential for maintenance of biologic function of the HA in the TB-HA hydrogels was assessed through fluorescent staining with b-HABP, which requires approximately twenty consecutive unmodified HA disaccharides [48] for binding. As seen in the inset in Fig. 9, the low level of substitution of HA in the TB-HA hydrogels allows for staining and visualization of the hydrogels by b-HABP. The folds seen on the image are a result of manual wrinkling of the hydrogel to introduce some three dimensional structure so as to allow for better visualization as the staining is very uniform throughout the hydrogel volume. The results indicate that physiologically relevant stretches (~20 consecutive disaccharides) of the TS-HA remain chemically unaltered, and therefore potentially available to participate in normal biologic processes.

4 Conclusions

The TB-HA hydrogels described in this manuscript possess many of the properties required for tissue engineering applications. Methods have been identified that provide for definitive characterization and quantification of the products of both the substitution (step 1) and cross-linking (step 2) reactions required for hydrogel formation including NMR spectroscopy, FACE analyses and those based on the spectrophotometric and fluorescent properties of the tyramine and dityramine adducts. The relatively stabile nature of the hydrogels to hyaluronidase digestion was demonstrated, which when combined with the stabile nature of the amide and carbon-carbon bonds involved in hydrogel formation, support previous observations of in vivo TB-HA hydrogel stability [25]. The non-cytotoxic nature of the HRP cross-linking process and the TB-HA hydrogel materials were also reported. The existence of HA, tyramine and peroxidase in normal mammalian tissues as well as the preservation of the majority of the native HA structure presumably contribute to the overall biocompatibility demonstrated by the TB-HA hydrogels in this and previous studies [25, 26]. As a result of the low percent tyramine substitution of HA carboxyl groups required for formation of stabile hydrogel constructs, the TB-HA hydrogel scaffolds described in this study provide the opportunity for normal biologic interaction in vivo as illustrated by their staining with b-HABP, a functional HA binding complex found in cartilage. Preservation of much of the negative charge contributed by the carboxyl groups in HA is predicted to preserve the contribution of HA to tissue physiomechanical properties.

Acknowledgements The authors would like to thank the Mizutani Foundation for Glycoscience and the Cleveland Clinic for their generous financial support. The authors would also like to acknowledge Christine Harris, Christine Roche, and Melanie Moore for their technical assistance, and Dr. Thomas Gerkin for his contribution to the NMR data.

References

1. C. Vinatier, J. Guicheux, G. Daculsi, P. Layrolle, P. Weiss, Biomed. Mater. Eng. **16**, S107 (2006)
2. J.K. Suh, H.W. Matthew, Biomaterials **21**, 2589 (2000). doi:10.1016/S0142-9612(00)00126-5
3. P. Angele, R. Kujat, M. Nerlich, J. Yoo, V. Goldberg, B. Johnstone, Tissue Eng. **5**, 545 (1999). doi:10.1089/ten.1999.5.545
4. T.C. Laurent, U.B. Laurent, J.R. Fraser, Immunol. Cell Biol. **74**, A1 (1996). doi:10.1038/icb.1996.32
5. V. Gupta, J.A. Werdenberg, T.L. Blevins, K.J. Grande-Allen, Tissue Eng. **13**, 41 (2007). doi:10.1089/ten.2006.0091
6. W.S. Turner, E. Schmelzer, R. McClelland, E. Wauthier, W. Chen, L.M. Reid, J. Biomed. Mater. Res. B: Appl. Biomater. **82**, 156 (2007). doi:10.1002/jbm.b.30717
7. X. Jia, Y. Yeo, R.J. Clifton, T. Jiao, D.S. Kohane, J.B. Kobler et al., Biomacromolecules **7**, 3336 (2006). doi:10.1021/bm060 4956
8. Y. Luo, K.R. Kirker, G.D. Prestwich, Modification of natural polymers: hyaluronic acid, ed. by A. Atala, R. Lanza, in *Methods of Tissue Engineering* (Academic Press, San Diego, 2001), pp. 539–553
9. N.E. Larsen, C.T. Pollak, K. Reiner, E. Leshchiner, E.A. Balazs, J. Biomed. Mater. Res. **27**, 1129 (1993). doi:10.1002/jbm.820 270903
10. L. Benedetti, R. Cortivo, T. Berti, A. Berti, F. Pea, M. Mazzo et al., Biomaterials **14**, 1154 (1993). doi:10.1016/0142-9612 (93)90160-4
11. J.J. Young, K.M. Cheng, T.L. Tsou, H.W. Liu, H.J. Wang, J. Biomater. Sci. Polym. Ed. **15**, 767 (2004). doi:10.1163/ 156856204774196153
12. D.L. Nettles, T.P. Vail, M.T. Morgan, M.W. Grinstaff, L.A. Setton, Ann. Biomed. Eng. **32**, 391 (2004). doi:10.1023/B:AB ME.0000017552.65260.94

13. X.Z. Shu, Y. Liu, Y. Luo, M.C. Roberts, G.D. Prestwich, Biomacromolecules **3**, 1304 (2002). doi:10.1021/bm025603c
14. J.L. Vanderhooft, B.K. Mann, G.D. Prestwich, Biomacromolecules **8**, 2883 (2007). doi:10.1021/bm0703564
15. J. Luo, C. Pardin, X.X. Zhu, W.D. Lubell, J. Comb. Chem. **9**, 582 (2007). doi:10.1021/cc060132+
16. R.N. Chen, H.O. Ho, M.T. Sheu, Biomaterials **26**, 4229 (2005). doi:10.1016/j.biomaterials.2004.11.012
17. E.P. Broderick, D.M. O'Halloran, Y.A. Rochev, M. Griffin, R.J. Collighan, A.S. Pandit, J. Biomed. Mater. Res. B: Appl. Biomater. **72**, 37 (2005). doi:10.1002/jbm.b.30119
18. M.E. Jones, P.B. Messersmith, Biomaterials **28**, 5215 (2007). doi:10.1016/j.biomaterials.2007.08.026
19. T.J. Sanborn, P.B. Messersmith, A.E. Barron, Biomaterials **23**, 2703 (2002). doi:10.1016/S0142-9612(02)00002-9
20. S. Sakai, K. Kawakami, Acta Biomater. **3**, 495 (2007). doi:10.1016/j.actbio.2006.12.002
21. R. Jin, C. Hiemstra, Z. Zhong, J. Feijen, Biomaterials **28**, 2791 (2007). doi:10.1016/j.biomaterials.2007.02.032
22. Y. Ogushi, S. Sakai, K. Kawakami, J. Biosci. Bioeng. **104**, 30 (2007). doi:10.1263/jbb.104.30
23. S.J. Sophia, A. Singh, D.L. Kaplan, J. Macromol. Sci, Part A **39**, 1151 (2002)
24. B. Kalra, A. Kumar, R.A. Gross, Polym. Reprints **41**, 1805 (2000)
25. J. Chan, A. Darr, D. Alam, A. Calabro, Am. J. Cosmet. Surg. **22**, 105 (2005)
26. K. Kamohara, M. Banbury, A. Calabro, Z.B. Popovic, A. Darr, Y. Ootaki et al., Heart Surg. Forum **9**, 888 (2006). doi:10.1532/HSF98.20061075
27. M. Kurisawa, J.E. Chung, Y.Y. Yang, S.J. Gao, H. Uyama, Chem. Commun. (Camb.), 4312 (2005). doi:10.1039/b506989 k
28. N. Blumenkrantz, G. Asboe-Hansen, Anal. Biochem. **54**, 484 (1973). doi:10.1016/0003-2697(73)90377-1
29. A. Calabro, M. Benavides, M. Tammi, V.C. Hascall, R.J. Midura, Glycobiology **10**, 273 (2000). doi:10.1093/glycob/10.3.273
30. A. Calabro, V.C. Hascall, R.J. Midura, Glycobiology **10**, 283 (2000). doi:10.1093/glycob/10.3.283
31. A. Calabro, R. Midura, A. Wang, L. West, A. Plaas, V.C. Hascall, Osteoarthr. Cartilage **9**(Suppl A), S16 (2001)
32. A. Calabro, V.C. Hascall, B. Caterson, Arch. Biochem. Biophys. **298**, 349 (1992). doi:10.1016/0003-9861(92)90421-R
33. W. Selbi, C. de la Motte, V. Hascall, A. Phillips, J. Am. Soc. Nephrol. **15**, 1199 (2004). doi:10.1097/01.ASN.0000125619.27422.8E
34. A. Wang, V.C. Hascall, J. Biol. Chem. **279**, 10279 (2004). doi:10.1074/jbc.M312045200
35. M. Aslam, A. Dent, *Bioconjugation: Protein Coupling Techniques for the Biomedical Sciences* (Macmillan Reference Ltd., London, 1998)
36. D. Sehgal, I.K. Vijay, Anal. Biochem. **218**, 87 (1994). doi:10.1006/abio.1994.1144
37. Q.P. Lei, D.H. Lamb, A.G. Shannon, X. Cai, R.K. Heller, M. Huang et al., J. Chromatogr. B: Anal. Technol. Biomed. Life Sci. **813**, 103 (2004). doi:10.1016/j.jchromb.2004.09.015
38. T. Matsumoto, E.E. Nieuwenhuis, R.L. Cisneros, B. Ruiz-Perez, K. Yamaguchi, R.S. Blumberg et al., J. Med. Microbiol. **53**, 97 (2004). doi:10.1099/jmm.0.05386-0
39. B. Ruiz-Perez, R.L. Cisneros, T. Matsumoto, R.J. Miller, G. Vasios, P. Calias et al., J. Infect. Dis. **188**, 378 (2003). doi:10.1086/376556
40. S.M. Holmbeck, P.A. Petillo, L.E. Lerner, Biochemistry **33**, 14246 (1994). doi:10.1021/bi00251a037
41. A.J. Gross, I.W. Sizer, J. Biol. Chem. **234**, 1611 (1959)
42. K.G. Welinder, Biochim. Biophys. Acta **1080**, 215 (1991)
43. M.D. Berry, J. Neurochem. **90**, 257 (2004). doi:10.1111/j.1471-4159.2004.02501.x
44. S.O. Andersen, Insect Biochem. Mol. Biol. **34**, 459 (2004). doi:10.1016/j.ibmb.2004.02.006
45. T.G. Huggins, M.W. Staton, D.G. Dyer, N.J. Detorie, M.D. Walla, J.W. Baynes et al., Ann. NY Acad. Sci. **663**, 436 (1992). doi:10.1111/j.1749-6632.1992.tb38692.x
46. U. auf dem Keller, A. Kumin, S. Braun, S. Werner, J. Invest. Dermatol. Symp. Proc. **11**, 106 (2006). doi:10.1038/sj.jidsymp.5650001
47. K.J. Davies, Biochem. Soc. Symp. **61**, 1 (1995)
48. L.L. Faltz, C.B. Caputo, J.H. Kimura, J. Schrode, V.C. Hascall, J. Biol. Chem. **254**, 1381 (1979)